Electronic Supporting Information

Constitutional Isomers of Carbazole-Benzoyl-Pyrimidine-Based Thermally Activated Delayed Fluorescence Emitters for Efficient OLEDs

Jayabalan Pandidurai,[+a] Jayachandran Jayakumar,[+a] Yi-Kuan Chen,[a] Chia-Min Hsieh,[a] and Chien-Hong Cheng*[ab]

[a]Department of Chemistry, National Tsing Hua University No. 101, Sec. 2, Kuang-Fu Rd., Hsinchu 30013, Taiwan
[b]Department of Chemistry, National Sun Yat-sen University, Kaohsiung, 80424, Taiwan

[+]These authors contributed equally

Email: chcheng@mx.nthu.edu.tw

Keywords: benzoyl-pyrimidine, π-π interaction, TADF, carbazole, OLEDs

General Information

^{1}H NMR and ^{13}C NMR spectra were measured on a Mercury 400 spectrometer. UV-vis absorption spectra were recorded on a Hitachi U-3300 spectrophotometer. Fluorescence and Phosphorescence spectra were recorded on a Hitachi F-7000 fluorescence spectrophotometer. The absolute photoluminescence quantum efficiencies (PLQYs) of the doped films were determined using an integrating sphere under an N_2 atmosphere. The thermogravimetric analysis (TGA) and differential scanning calorimetry (DSC) were performed on a thermal analyzer (2-HT, Mettler-Toledo) at a heating rate of 10 °C/min. from 30 °C to 800 °C under nitrogen. Transient PL decay measurements were done using an Edinburgh FLS 980 instrument. The HOMO levels of the emitters in the neat film were determined by a Riken Keiki AC-2 photoelectron spectrometer with a UV source. The X-ray diffraction was carried out on an X-ray diffractometer (X8 APEX, Bruker).

DFT Calculation

Molecular geometry optimizations and electronic properties of these materials were carried out by using the Gaussian 09 program with density functional theory (DFT) and time-dependent DFT (TD-DFT for S_1 and T_1 states) calculations in which the Becke's three-parameter functional combined with Lee, Yang, and Parr's correlation functional (B3LYP) hybrid exchange-correlation functional with the 6-31G (d,p) basis set was used.[1] The molecular orbitals were visualized by Gaussview 5.0 software.[1,2] All calculations were performed in the gas phase.

OLEDs Fabrication and Measurement

Organic materials used in device fabrication were purified by sublimation. Devices were fabricated by vacuum deposition onto pre-coated ITO glasses with a sheet resistance of 15 Ω/square at a pressure lower than 10^{-6} Torr. Organic materials were deposited at the rate of 0.5~1.2 Å s^{-1}. LiF and Al were deposited at the rate of 0.1 Å s^{-1} and 3-10 Å s^{-1}, respectively. The rest of the procedures is similar to the reported method.[3] Current-voltage-luminance (I-V-L) characterization and electroluminescent spectra were measured and recorded by using a programmable source meter (2400, Keithley) and a spectroradiometer (CS2000A, Konica Minolta). External quantum efficiencies and power efficiencies were determined by the Lambertian emission device assumption.
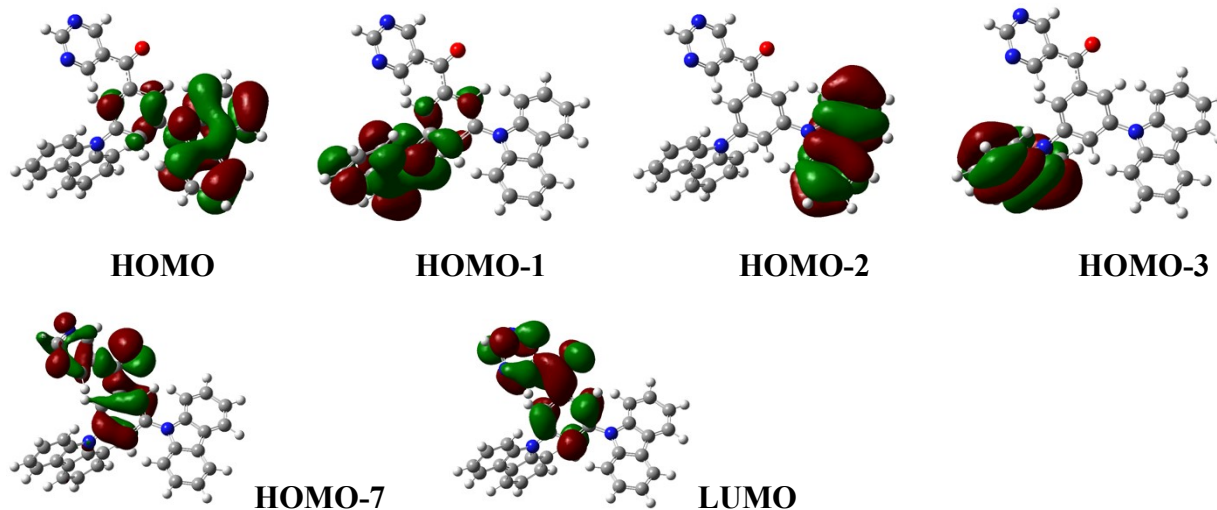
Table S1. Singlet and triplet excitation states, and transition configurations of the 35CzBPym by TD-DFT at the B3LYP/6-31G (d,p).

State	Excitation		E_{cal} (eV)[a]	λ_{cal} (nm)[b]	f[c]
	Singlet Excited States				
S_1	HOMO-1 → LUMO	-0.21432	2.6258	472	0.0090
	HOMO → LUMO	0.67011			
S_2	HOMO-1 → LUMO	0.67097	2.6739	463	0.0054
	HOMO → LUMO	0.21443			
S_3	HOMO-2 → LUMO	0.70505	3.0049	412	0.0000
S_4	HOMO-3 → LUMO	0.70592	3.0342	408	0.0001
	Triplet Excited States				
T_1	HOMO-1 → LUMO	-0.27494	2.5055	494	
	HOMO → LUMO	0.63232			-
T_2	HOMO-1 → LUMO	0.62485	2.5626	483	
	HOMO → LUMO	0.26538			-
T_3	HOMO-7 → LUMO	0.65404	2.9219	424	
					-
T_4	HOMO-2 → LUMO	0.7029	3.0035	412	

S_1-T_1 = ΔE_{ST} 2.6258 − 2.5055 = 0.1203 eV

[a]Excitation energy; [b]excitation wavelength (λ); [c]oscillator strength (f).

HOMO   **HOMO-1**   **HOMO-2**   **HOMO-3**
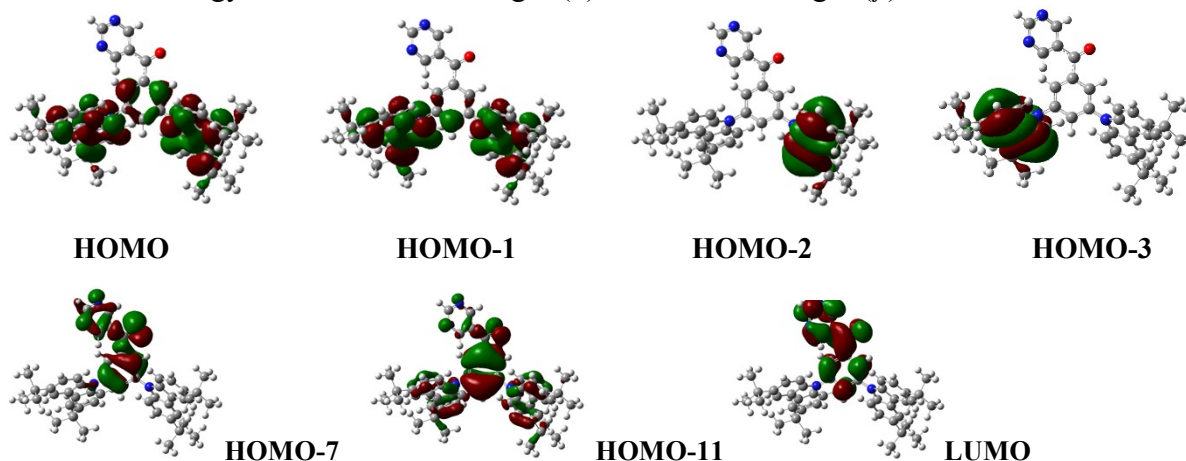

HOMO-7   **LUMO**

Table S2. Singlet and triplet excitation states, and transition configurations of the 35tCzBPym by TD-DFT at the B3LYP/6-31G (d,p).

State	Excitation		E_{cal} (eV)[a]	λ_{cal} (nm)[b]	f[c]
	Singlet Excited States				
S_1	HOMO → LUMO	0.70353	2.4703	501	0.0161
S_2	HOMO-1 → LUMO	0.70345	2.5961	477	0.0051
S_3	HOMO-3 → LUMO	0.70592	2.8964	428	0.0002
S_4	HOMO-2→ LUMO	0.70504	3.4853	427	0.0000
	Triplet Excited States				
T_1	HOMO → LUMO	0.69111	2.3599	525	-
T_2	HOMO-11 → LUMO	-0.10550	2.4281	494	-
	HOMO-1 → LUMO	0.68484			
T_3	HOMO-7 → LUMO	-0.22924	2.9208	428	-
	HOMO-3 → LUMO	0.64705	3.0035		
	HOMO-2 → LUMO	-0.12095			
T_4	HOMO-3 → LUMO	0.13478	2.9162	425	-
	HOMO-2 → LUMO	0.68929			

S_1-T_1 = ΔE_{ST} 2.4703 − 2.3599 = 0.110 eV

[a]Excitation energy; [b]excitation wavelength (λ); [c]oscillator strength (f).

HOMO   **HOMO-1**   **HOMO-2**   **HOMO-3**
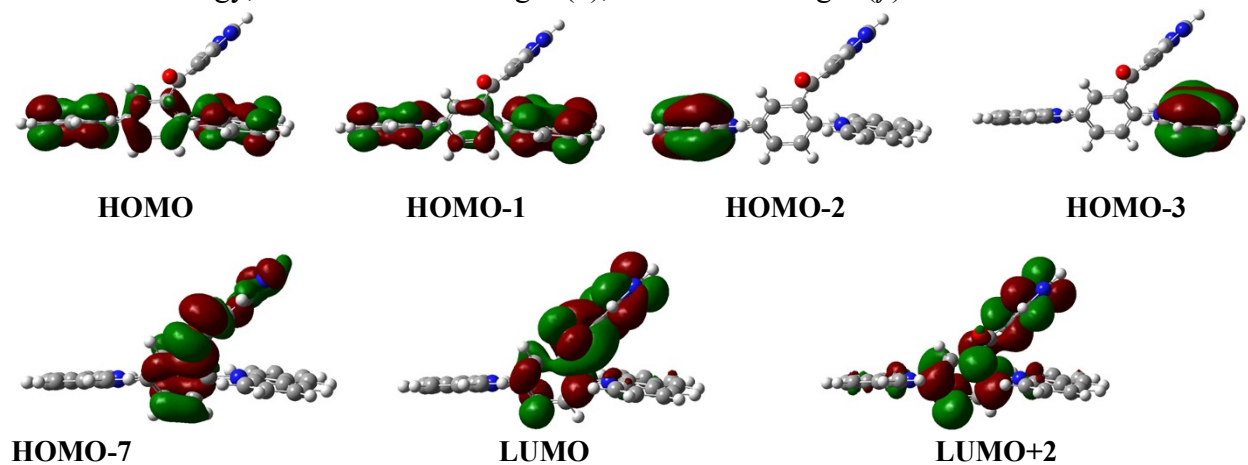
HOMO-7   **HOMO-11**   **LUMO**

Table S3. Singlet and triplet excitation states, and transition configurations of the 25CzBPym by TD-DFT at the B3LYP/6-31G (d,p).

State	Excitation	E_{cal} (eV)[a]	λ_{cal} (nm)[b]	f[c]
	Singlet Excited States			
S_1	HOMO-1 → LUMO HOMO → LUMO	-0.20549 0.67332	2.6259	472	0.0210
S_2	HOMO-1 → LUMO HOMO → LUMO	0.67233 0.20549	2.9200	424	0.0004
S_3	HOMO-3 → LUMO	0.70550	3.0813	402	0.0031
S_4	HOMO-2 → LUMO	0.70512	3.2000	387	0.0000
	Triplet Excited States			
T_1	HOMO-7 → LUMO HOMO-1 → LUMO HOMO → LUMO HOMO → LUMO+2	-0.10504 -0.18314 0.65611 0.10232	2.4991	496	-
T_2	HOMO-1 → LUMO HOMO → LUMO	0.66537 0.18097	2.8637	432	-
T_3	HOMO-7 → LUMO	0.64789	3.0081	412	-
T_4	HOMO-3 → LUMO	0.70110	3.0604	405	
	S_1-T_1 = ΔE_{ST}	2.6259 – 2.4991 = 0.126 eV			

[a]Excitation energy; [b]excitation wavelength (λ); [c]oscillator strength (f).

HOMO   **HOMO-1**   **HOMO-2**   **HOMO-3**

HOMO-7   **LUMO**   **LUMO+2**

Table S4. Singlet and triplet excitation states, and transition configurations of the 25tCzBPym by TD-DFT at the B3LYP/6-31G (d,p).

State	Excitation		E_{cal} (eV)[a]	λ_{cal} (nm)[b]	f[c]
	Singlet Excited States				
S_1	HOMO → LUMO	0.66554	2.5121	494	0.0324
S_2	HOMO-1 → LUMO	0.66258	2.7759	467	0.0055
S_3	HOMO-3 → LUMO	0.70572	2.9915	414	0.0060
S_4	HOMO-2 → LUMO	0.70520	3.0777	403	0.0000
	Triplet Excited States				
T_1	HOMO → LUMO	0.66023	2.4075	515	-
	HOMO-1 → LUMO	-0.20568			
					-
T_2	HOMO-7 → LUMO	0.17053	2.6982	460	
	HOMO-1 → LUMO	0.64344			-
	HOMO → LUMO	0.20025			
T_3	HOMO-3 → LUMO	0.69980	2.9656	418	-
T_4	HOMO-7 → LUMO	0.62094	3.0008	413	
	HOMO-1 → LUMO	-0.16335			
	HOMO → LUMO+2	-0.10496			

S_1-T_1 = ΔE_{ST} 2.5121 − 2.4075 = 0.1046 eV

[a]Excitation energy; [b]excitation wavelength (λ); [c]oscillator strength (f).

HOMO   HOMO-1   HOMO-2   HOMO-3

LUMO   LUMO+1
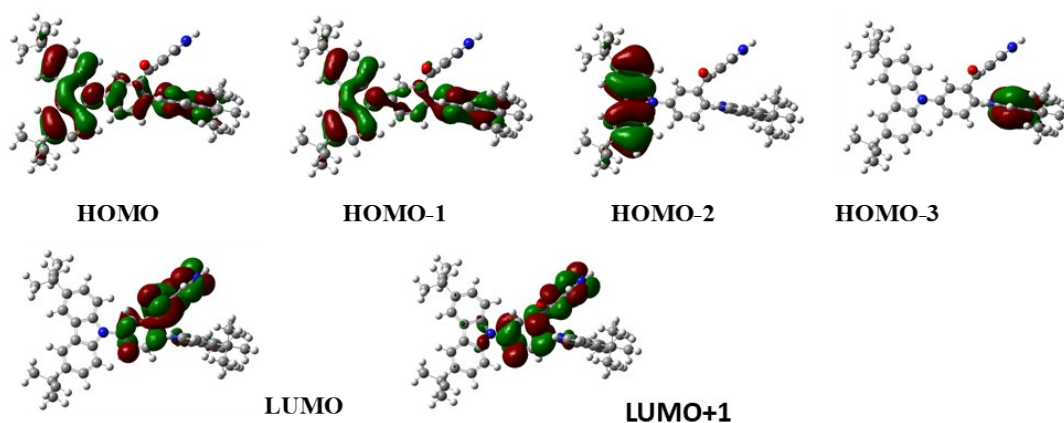
Table S5. Natural transition orbitals in the first singlet excitation states of the emitter.
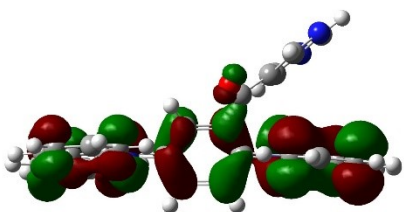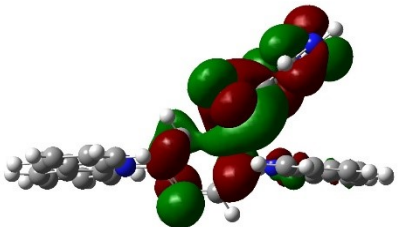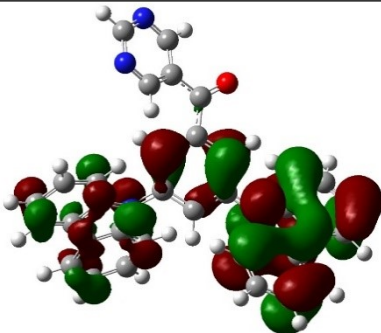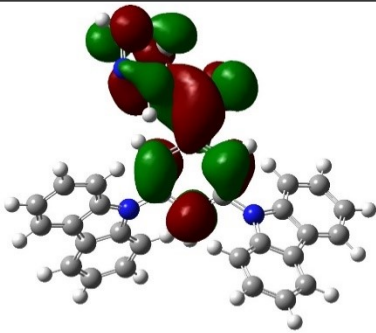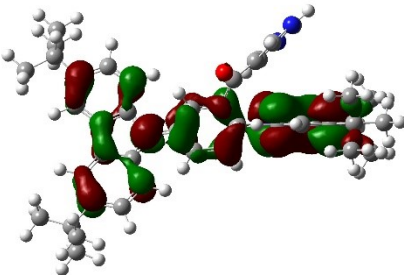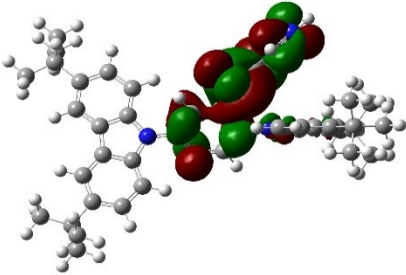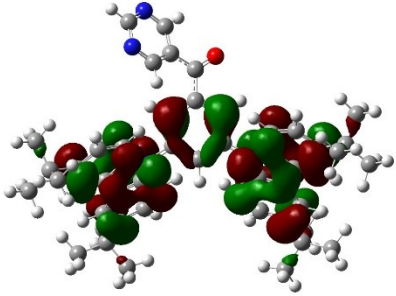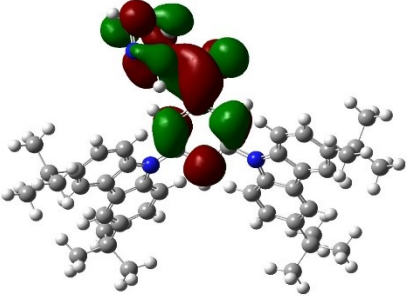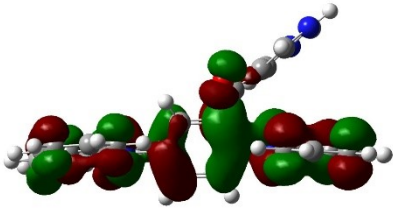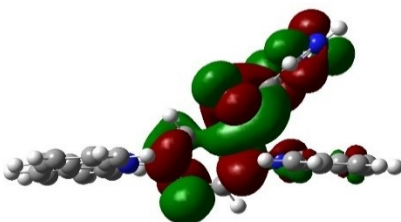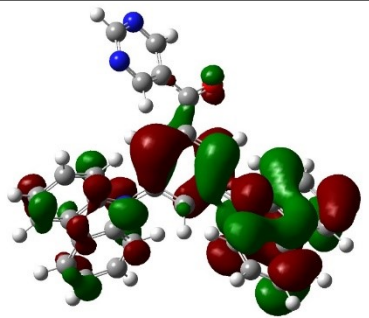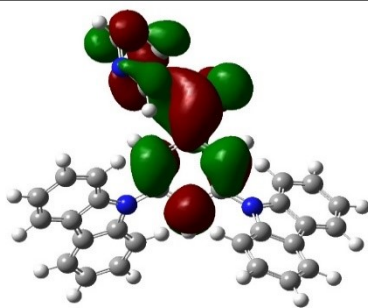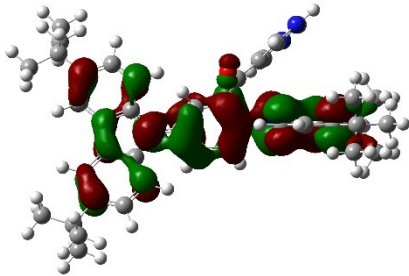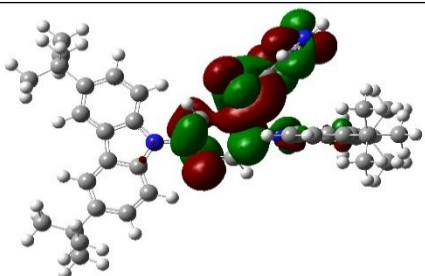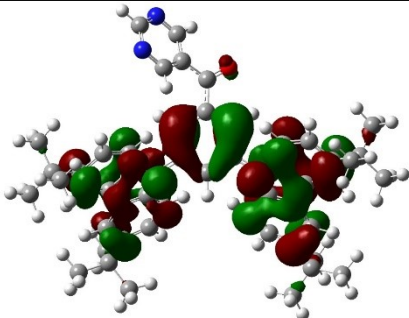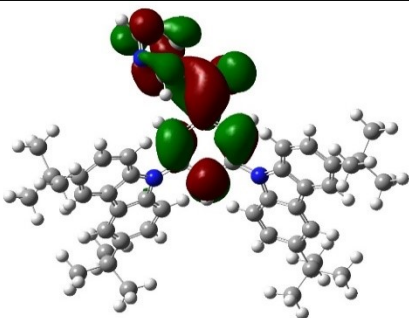
Emitter	Holes (S_1)	Particles (S_1)
25CzBPym		
35CzBPym		
25tCzBPym		
35tCzBPym		

Table S6. Natural transition orbitals in the first triplet excitation states of the emitter.

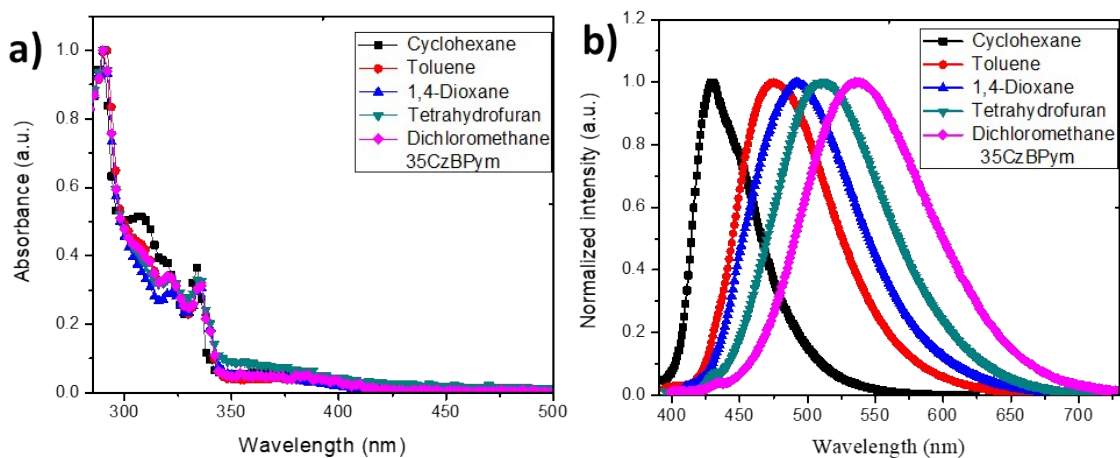| Emitter	Holes (T$_1$)	Particles (T$_1$)
25CzBPym		
35CzBPym		
25tCzBPym		
35tCzBPym		

Photophysical properties

Fig S1. a) Absorbance and b) fluorescence spectra of 35CzBPym in various solvents at RT (10^{-5} M).
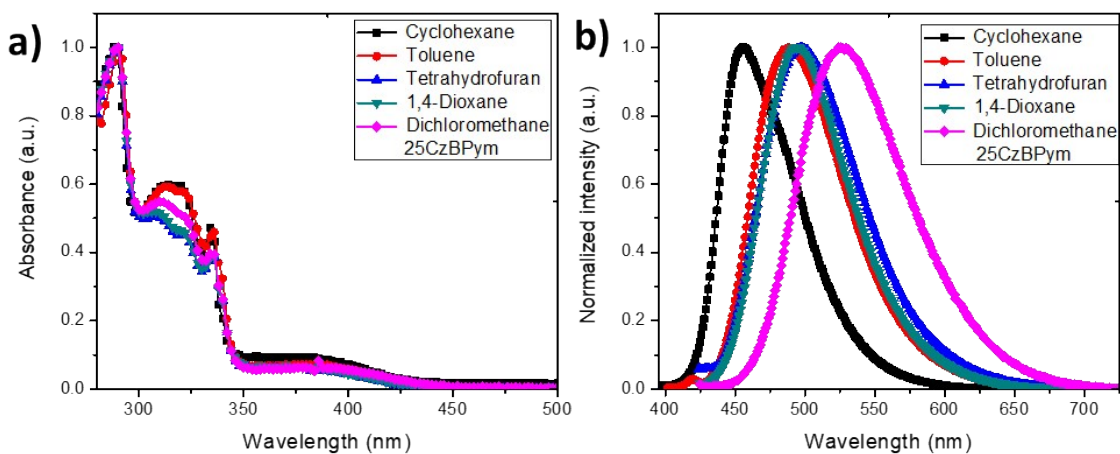

Fig S2. a) Absorbance and b) fluorescence spectra of 25CzBPym in various solvents at RT (10^{-5} M).
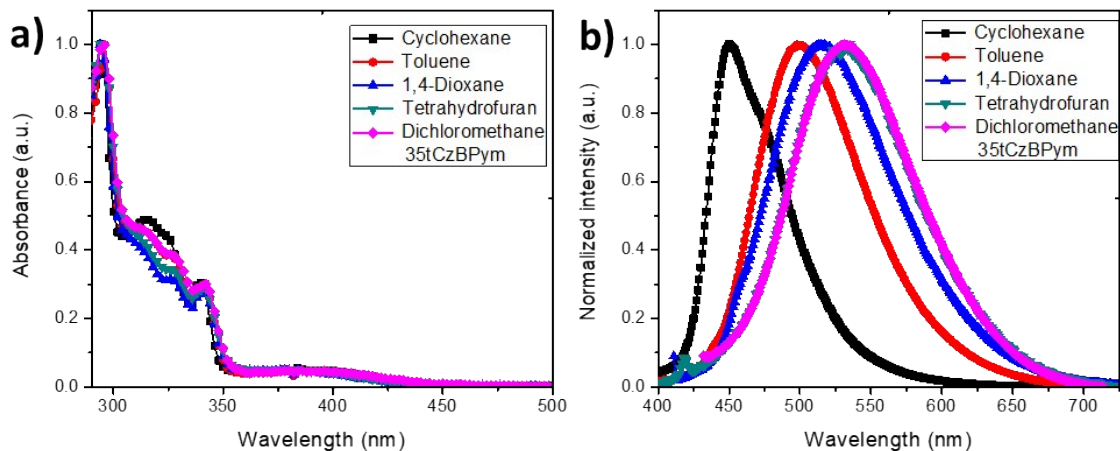
Fig S3. a) Absorbance and b) fluorescence spectra of 35tCzBPym in various solvents at RT (10^{-5} M).

Fi

g S4. a) Absorbance and b) fluorescence spectra of 25tCzBPym in various solvents at RT (10^{-5} M).
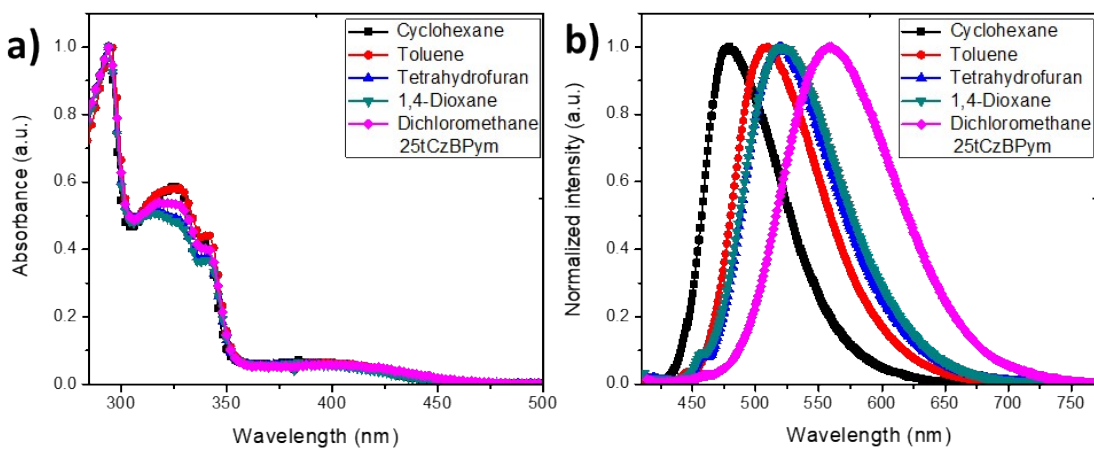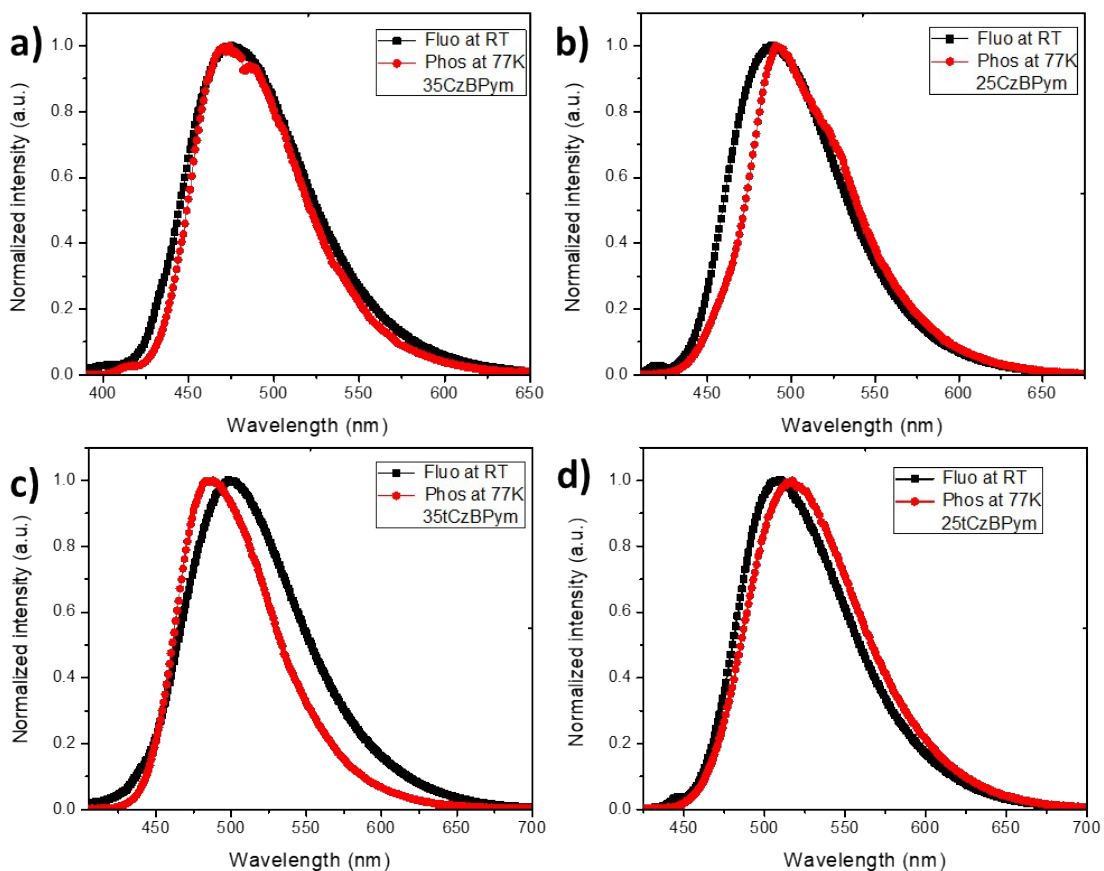
Fig S5. Fluorescence (Fluo.) spectra of a) 35CzBPym, b) 25CzBPym, c) 35tCzBPym, and d) 25tCzBPym in toluene (10^{-5} M) solution at room temperature and phosphorescence (Phos.) spectra in toluene (10^{-5} M) at 77 K.
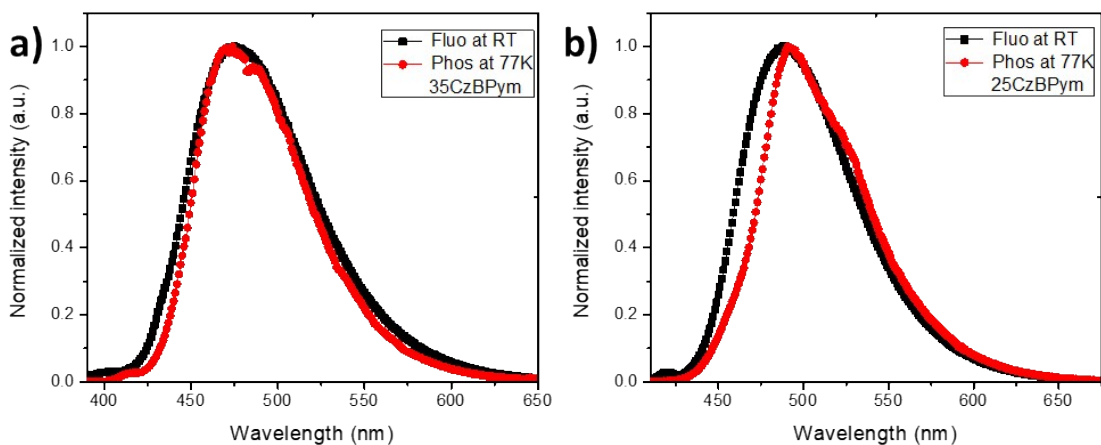
Fig S6. Fluorescence (Fluo.) and phosphorescence spectra of a) 35CzBPym and b) 25CzBPym doped in mCBP thin films (7 wt%).
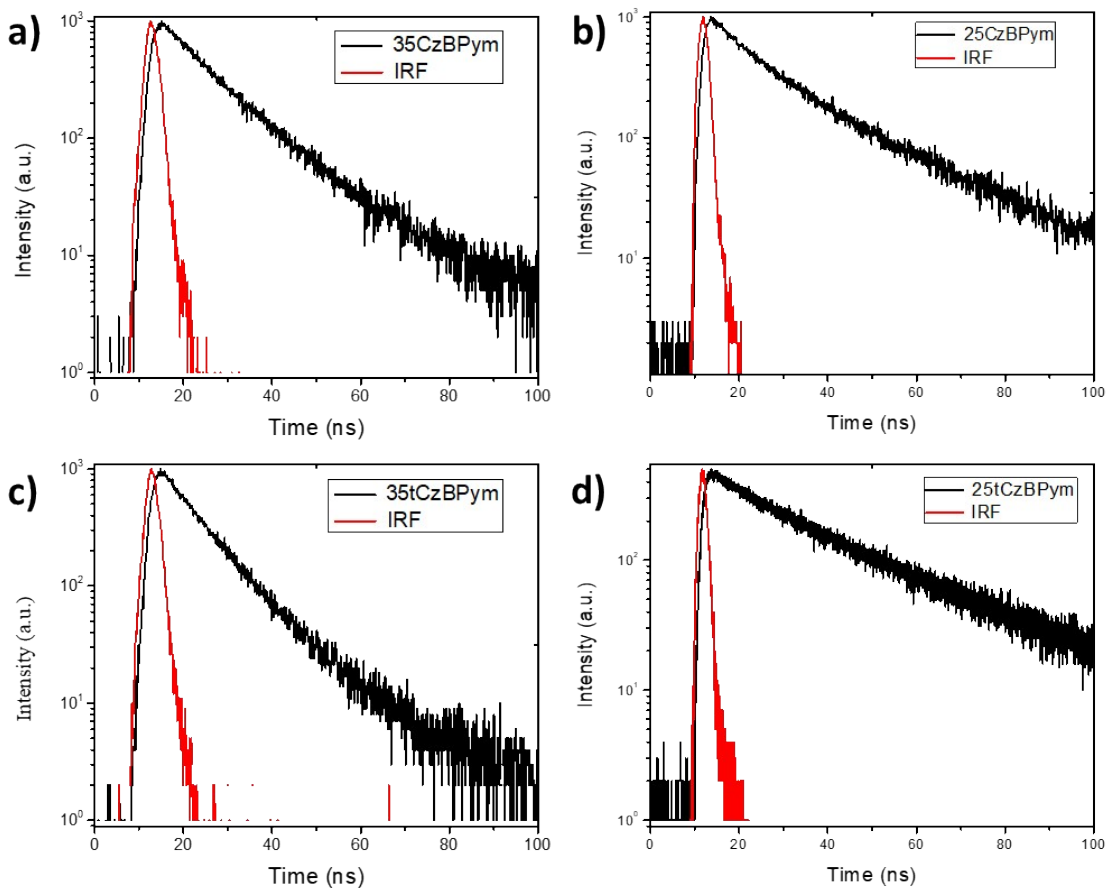
Fig S7. Prompt fluorescence spectra of a) 35CzBPym, b) 25CzBPym, c) 35tCzBPym, and d) 25tCzBPym doped in mCBP thin films (7 wt%) at 300 K.
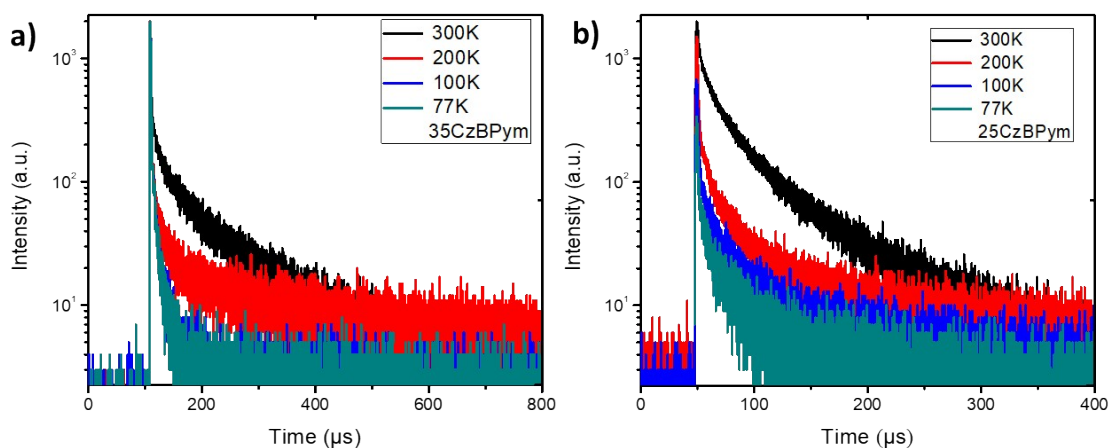
Fig S8. The transient PL decay curves of 7 wt% a) 35CzBPym and b) 25CzBPym doped in mCBP thin films at various temperatures.

Photoelectron spectroscopy and Thermal properties
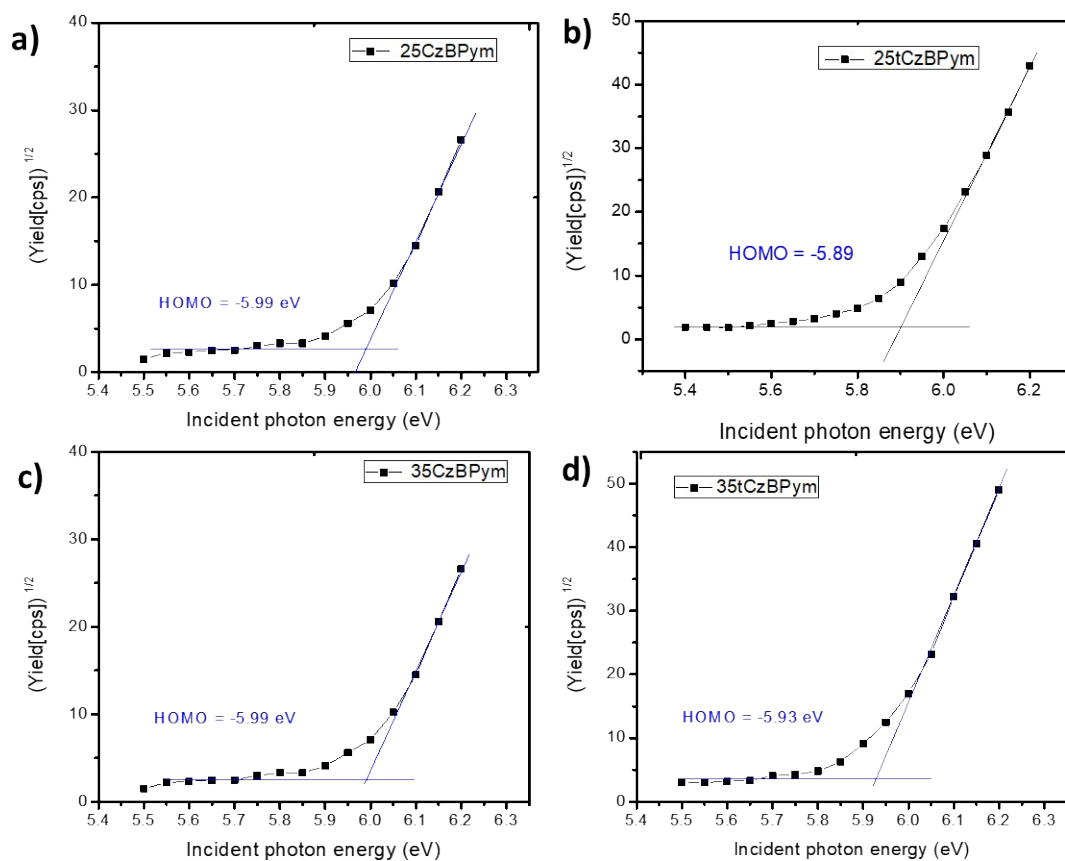
Fig S9. Photoelectron spectroscopy a) of 25CzBPym, b) 25tCzBPym, c) 35CzBPym, and d) 35tCzBPym measured in neat films.

Fig S10. The thermogravimetric analysis (TGA) of (a) 35CzBPym and 35tCzBPym and (b) 25CzBPym and 25tCzBPym. The differential scanning calorimetry (DSC) of (c) 35CzBPym and 35tCzBPym and (d) 25CzBPym and 25tCzBPym.

EL-properties of the devices

Chemical structures of the device materials

TAPC

mCBP

| Al (100 nm) |
| LiF (0.8 nm) |
| TmPyPB (60 nm) |
| mCBP : emitter (7% wt) (30nm) |
| TAPC (30 nm) |
| MoO3 (5 nm) |
| ITO |

TmPyPB

Fig S11. Structures of the materials used in the devices and schematic representation of the device

Table S7. Summarized doped-device optimization of emitters with different host matrix.
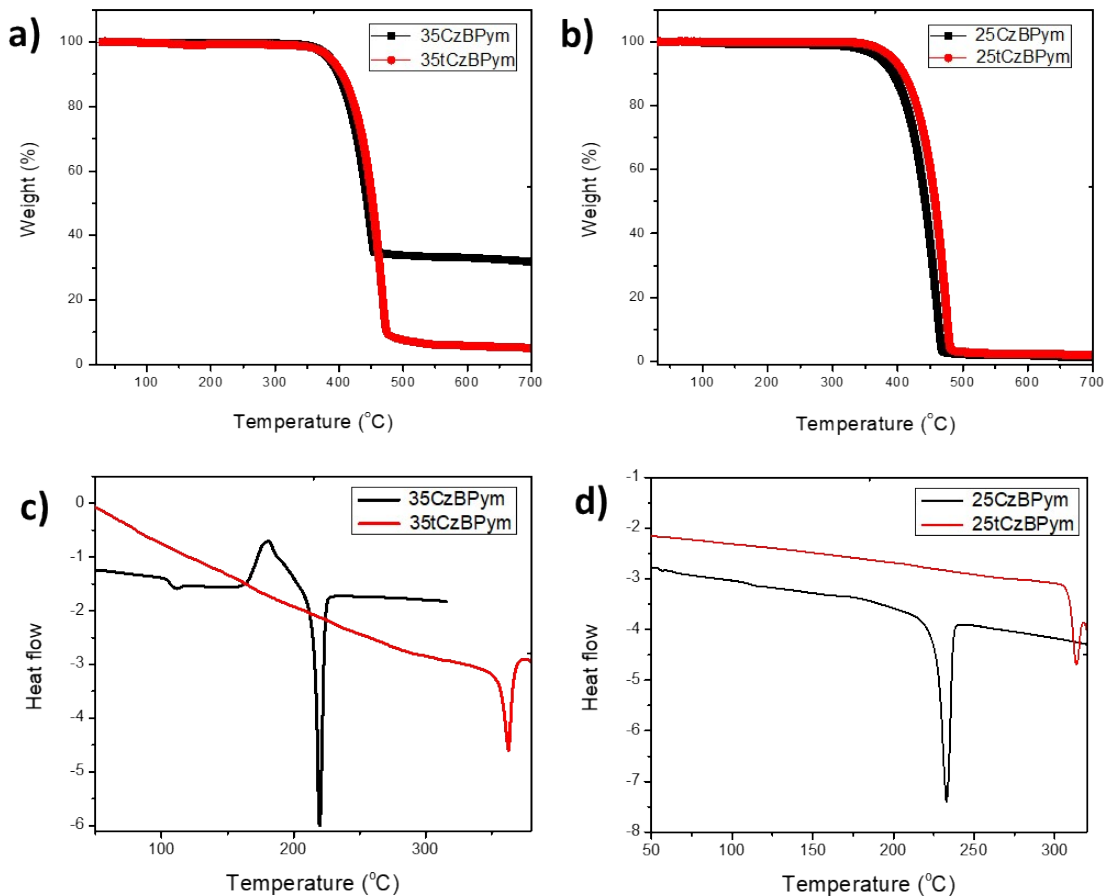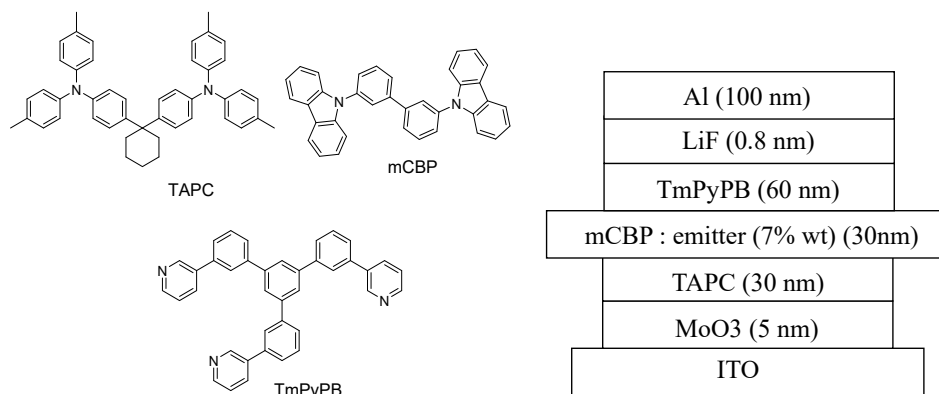

CBP

mCBP

mCPCN
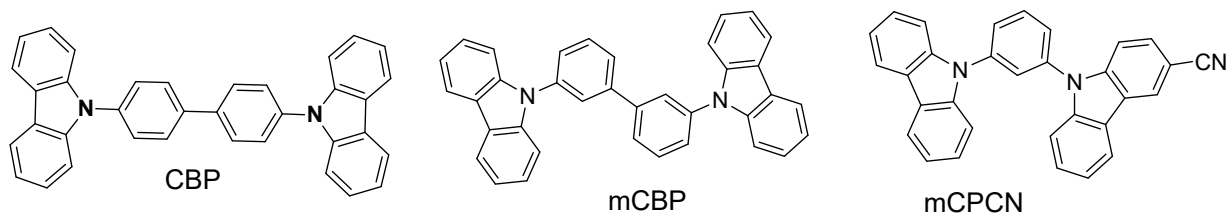
H1: ITO /MoO$_3$ (5)/TAPC (30)/CBP: 25tCzBPym (7 wt%) (30)/TmPyPB (60)/LiF (0.8)/Al (100)

H2: ITO /MoO$_3$ (5)/TAPC (30)/mCBP: 25tCzBPym (7 wt%) (30)/TmPyPB (60)/LiF (0.8)/Al (100)

H3: ITO /MoO$_3$ (5)/TAPC (30)/mCPCN: 25tCzBPym (7 wt%) (30)/TmPyPB (60)/LiF (0.8)/Al (100)

Anode: ITO Cathode: Al (100) (unit:nm)

Device	PLQY (%)[a]	V_{on} (V)[b]	L (cd m^{-2})[c]	EQE (%)[d]	λ_{max} (nm)[e]	CIE$_{(x, y)}$ at 8 V
H1	60	3.5	12502	15.9	492	(0.19, 0.38)
H2	88	3.7	32077	23.3	500	(0.20, 0.47)
H3	80	4.0	14093	20.1	504	(0.21, 0.48)

[a] PLQY, photoluminescence quantum yield of a 7 wt% BPym emitter doped film; [b] V_{on}, the operating voltage at a brightness of 1 cd m^{-2}; [c] L, maximum luminance; [d] EQE, maximum external quantum efficiency; [e] λ_{max}, the wavelength of the EL spectrum with maximum intensity at 8 V

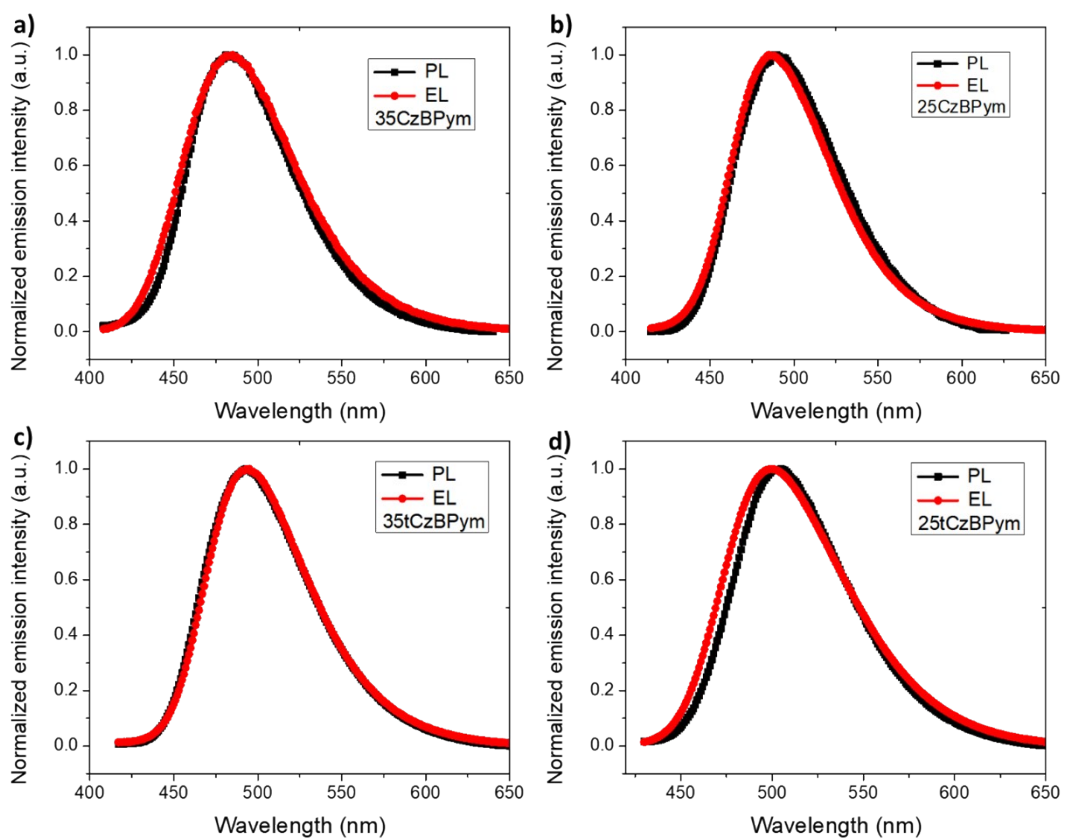**Fig S12.** Comparison of PL and EL-characteristics of emitters in doped thin-films (a-d)
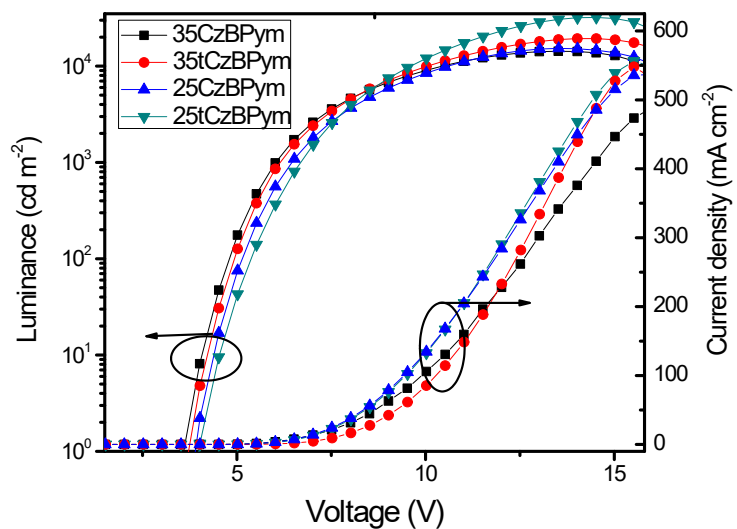

Fig S13. a) Luminance-voltage-current efficiency of 35CzBPym, 35tCzBPym, 25CzBPym, and 25tCzBPym -based devices.

Table S8. EL performances of representative blue to green pyrimidine-based TADF OLEDs.[a]

Entry	Blue-green Emitter	L_{max} (cd m^{-2})	EQE$_{max}$ (%)	EQE (%) at 1,000 cd m^{-2}	CIE (x, y)	EL$_{max}$ (nm)	Ref.
1	**35CzBPym**	**14286**	**13.5**	**9.1**	**(0.16, 0.30)**	**482**	**This work**
2	**25CzBPym**	**15278**	**15.3**	**8.7**	**(0.15, 0.34)**	**486**	
3	**35tCzBPym**	**19314**	**19.1**	**9.7**	**(0.17, 0.42)**	**494**	**This work**
4	**25tCzBPym**	**32077**	**23.3**	**13.6**	**(0.20, 0.47)**	**500**	
5	6,7-DCQx-Ca	-	21.5	-	(0.37, 0.57)	541	4a
6	CzPCN	13100	12.8	-	(0.20, 0.36)	494	4a
7	tCzPCN	13200	5.1	-	(0.19, 0.35)	490	4a
8	MeOCzPCN	9300	1.4	-	(0.30, 0.49)	524	4a
9	2PyCNICz	-	17.1	-	(0.31, 0.57)	-	4b
10	2PyCNBCz	-	14.5	-	(0.34, 0.58)	-	4b
11	Ac-HPM	-	20.9	11.7	(0.21, 0.44)	-	4c
12	Ac-PPM	-	19.0	11.2	(0.21, 0.44)	-	4c
13	Ac-MPM	-	24.5	10.1	(0.19, 0.37)	-	4c
14	MFAc-PPM	-	20.4	-	(0.16, 0.23)	470	4d
15	MXAc-PPM	-	12.2	-	(0.16, 0.20)	462	4d
16	MFAc-PM	-	17.1	-	(0.16, 0.21)	469	4d
17	MXAc-PM	-	14.3	-	(0.16,0.19)	460	4d
18	Ac-PM	-	11.4	-	(0.15,0.15)	458	4d
19	PXZPM	-	19.9	14.2	(0.33,0.57)	-	4e
20	PXZMePM	-	22.2	15.4	(0.30,0.56)	-	4e
21	PXZPhPM	-	24.6	18.2	(0.32,0.57)	-	4e
22	Ac-1MHPM	-	24.0	11.2	(0.17,0.28)	-	4f
23	Ac-2MHPM	-	19.8	9.6	(0.17,0.27)	-	4f
24	Ac-3MHPM	-	17.8	-	(0.16,0.15)	-	4f
25	Pm2	-	31.3	-	(0.32,0.59)	-	4g
26	Pm5	-	30.6	-	(0.32,0.57)	-	4g
27	Ac-46DPPM	-	11.8	-	(0.16,0.21)	-	4h
28	PXZ-PYR	4214	27.9	12.3	(0.35,0.56)	536	4i

29	PXZ-muPXR	22730	29.1	20.5	(0.32,0.55)	529	4i
30	PXZ-mdPYR	7762	27.5	16.5	(0.29,0.49)	514	4i
31	PXZ-2mPYR	12476	26.3	8.9	(0.23,0.42)	502	4i

[a] The results were obtained from reference.

References

1   C. Adamo and V. Barone, *J. Chem. Phys.*, 1999, **110**, 6158-6170.

2   a). M. Ernzerhof and G. E. Scuseria, *J. Chem. Phys.*, 1999, **110**, 5029-5036. b) Frisch, M. J. Gaussian   09, revision D.01; Gaussian, Inc.: Wallingford, CT, 2013.

3   I. S. Park, S. Y. Lee, C. Adachi and T. Yasuda, *Adv. Funct. Mater.*, 2016, **26**, 1813-1821.

4.   a) U. Tsiko, O. Bezvikonnyi, G. Sych R. Keruckiene, D. Volyniuk, J. Simokaitiene, I. Danyliv, Y. Danyliv, A. Bucinskas, X.Tan, and J. VidasGrazulevicius. Journal of Advanced Research 2021, **33**, 41–51; b)   J. S. Jang, H. L. Lee, J. Y. Lee, *J. Mater. Chem. C*, 2019, **7**, 12695-12703; c)   R. Komatsu, H. Sasabe, Y. Seino, K. Nakao and J. Kido, *J. Mater. Chem. C*, 2016, **4**, 2274–2278; d)   I. S. Park., H. Komiwamaa and T. Yasuda, *Chem. Sci.*, 2017, **8**, 953–960; e)   K. Wu, T. Zhang, L. Zhan, C. Zhong, S. Gong, N. Jiang, Z. H. Lu and C. Yang, Chem. – Eur. J., 2016, **22**, 10860–10866; f)   R. Komatsu, T. Ohsawa, H. Sasabe, K. Nakao, Y. Hayasaka and J. Kido, *ACS Appl. Mater. Interfaces*, 2017, **9**, 4742–4749; g)   K. Pan, S. Li, Y. Ho, Y. Shiu, W. Isai, M. Jiao, W. Lee, C. Wu, C. Chung, T. Chatteriee, Y. Li, K. Wong, H. Hu, C. Chen and M. Lee, *Adv. Funct. Mater*., 2016, **26**, 7560–7571; h) K. Nakao, H. Sasabe, J. Kido, *Adv. optical. Mater.*, 2017, **5**, 1600843; i) T. Serevicivs, R. Skaisgiris, S. Tumkeicivs and S. Jursenas, *ACS Appl. Mater. Interfaces*, 2012, **12**, 10727-10736.
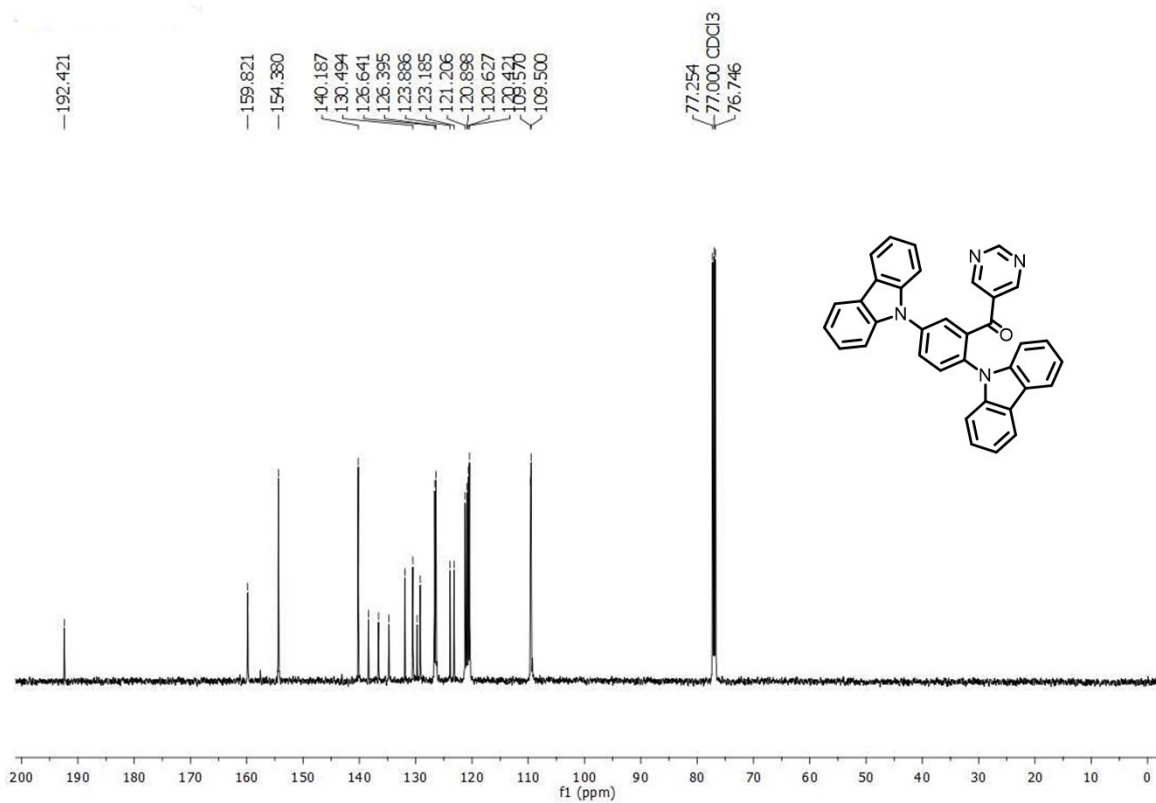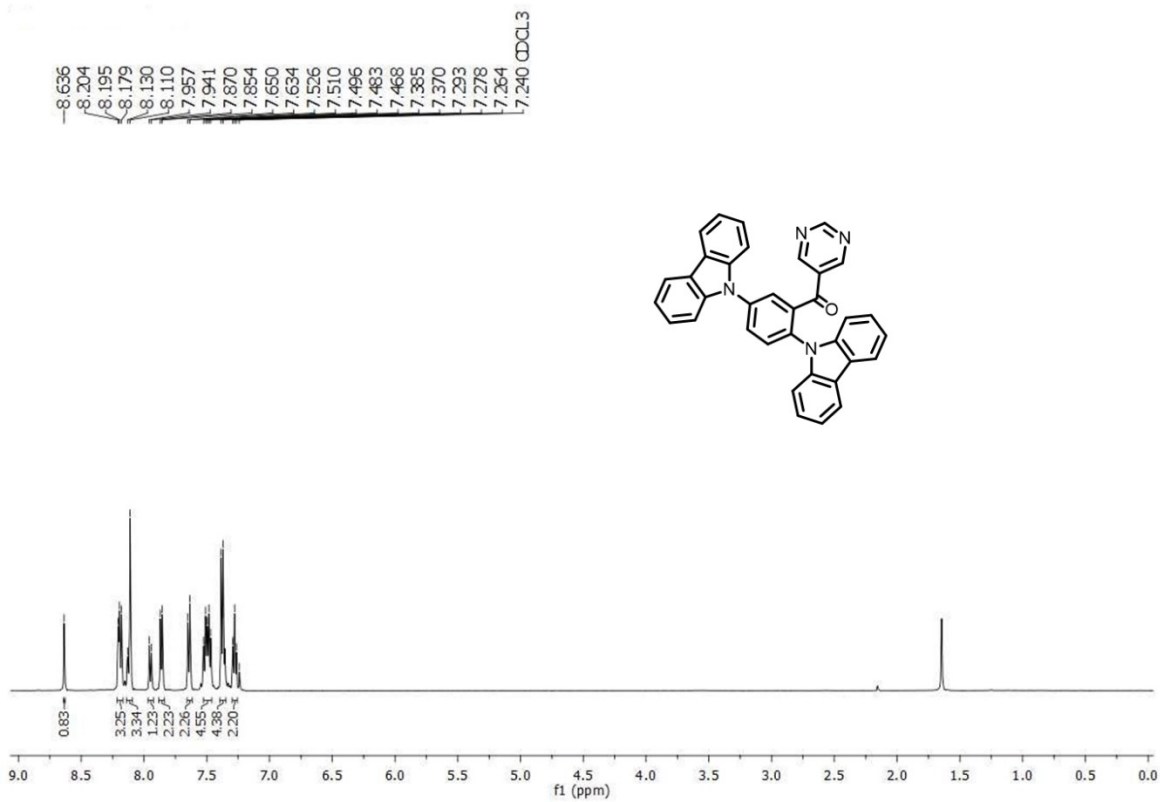
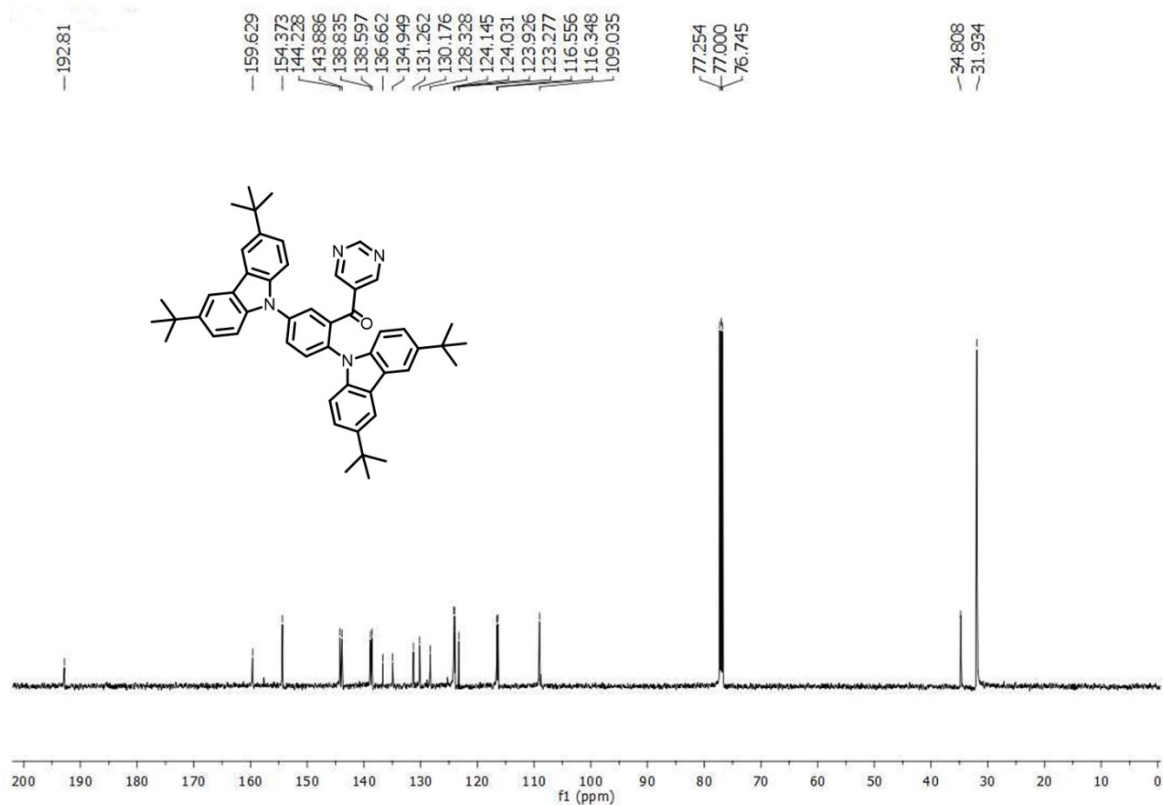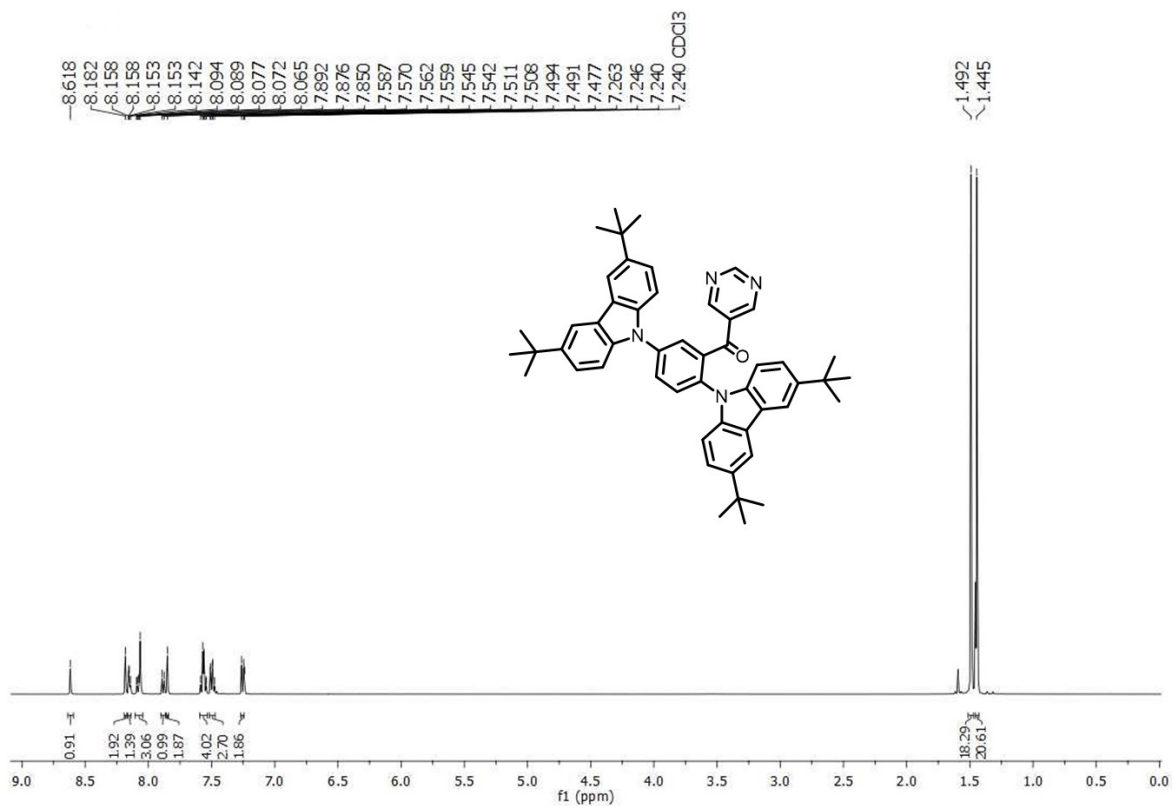# ¹H AND ¹³C Spectra of compound (35CzBPym)
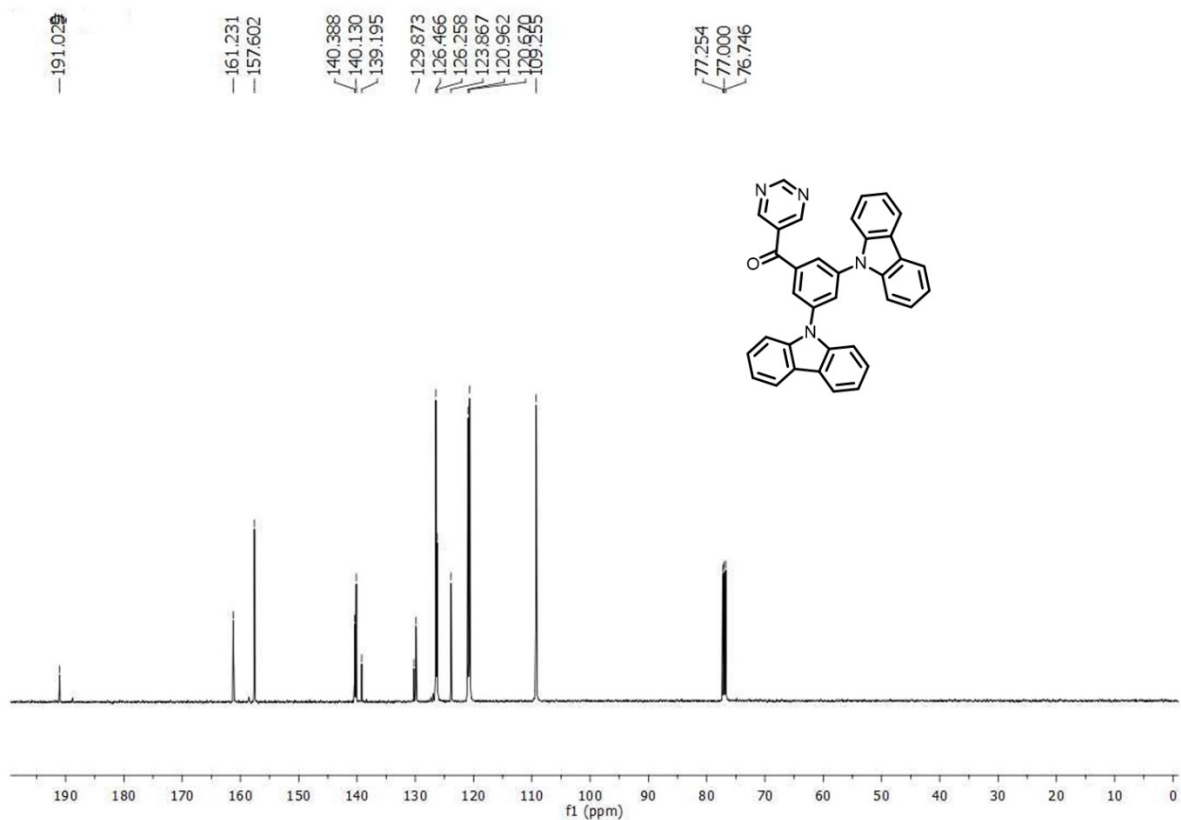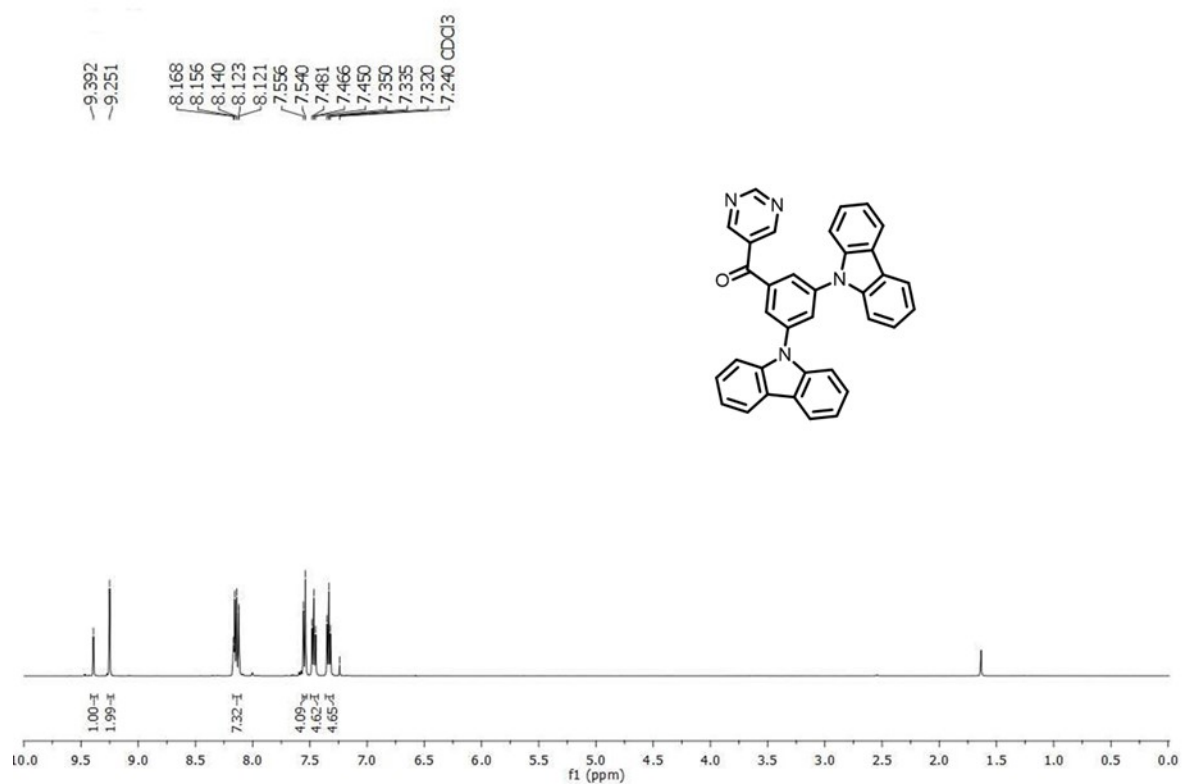
^{1}H AND ^{13}C Spectra of compound (35tCzBPym)
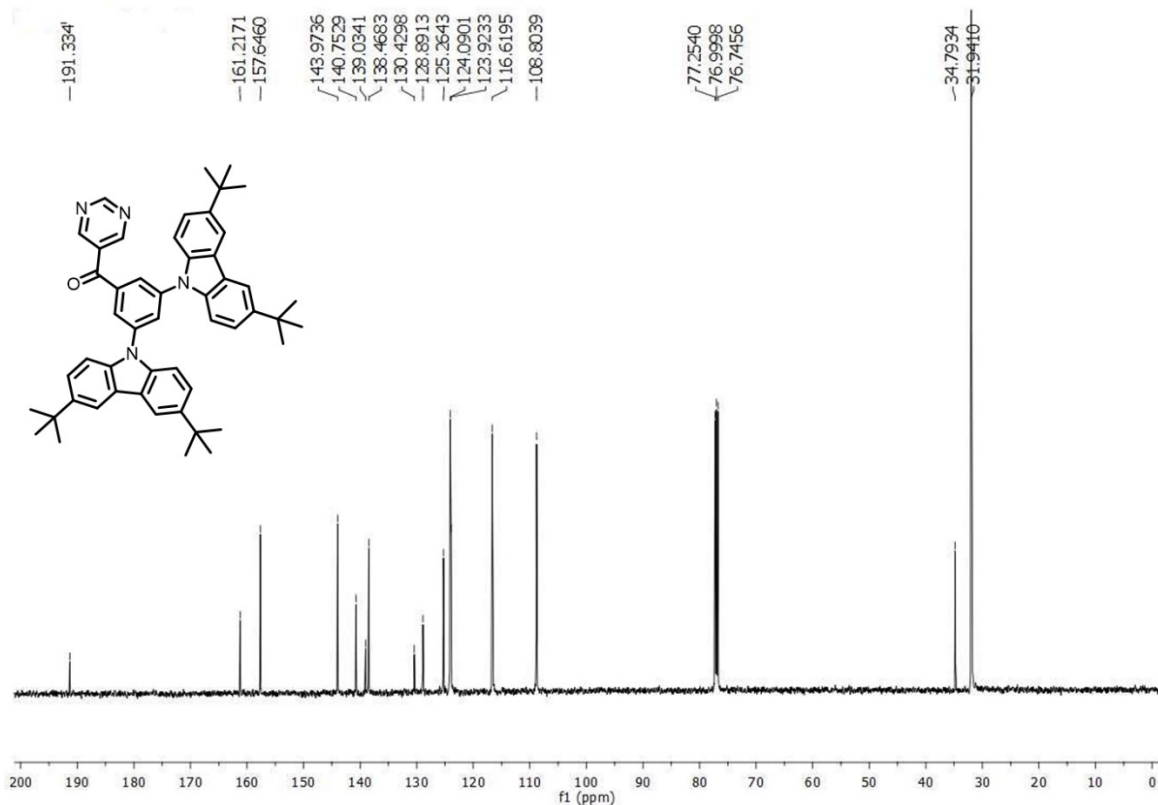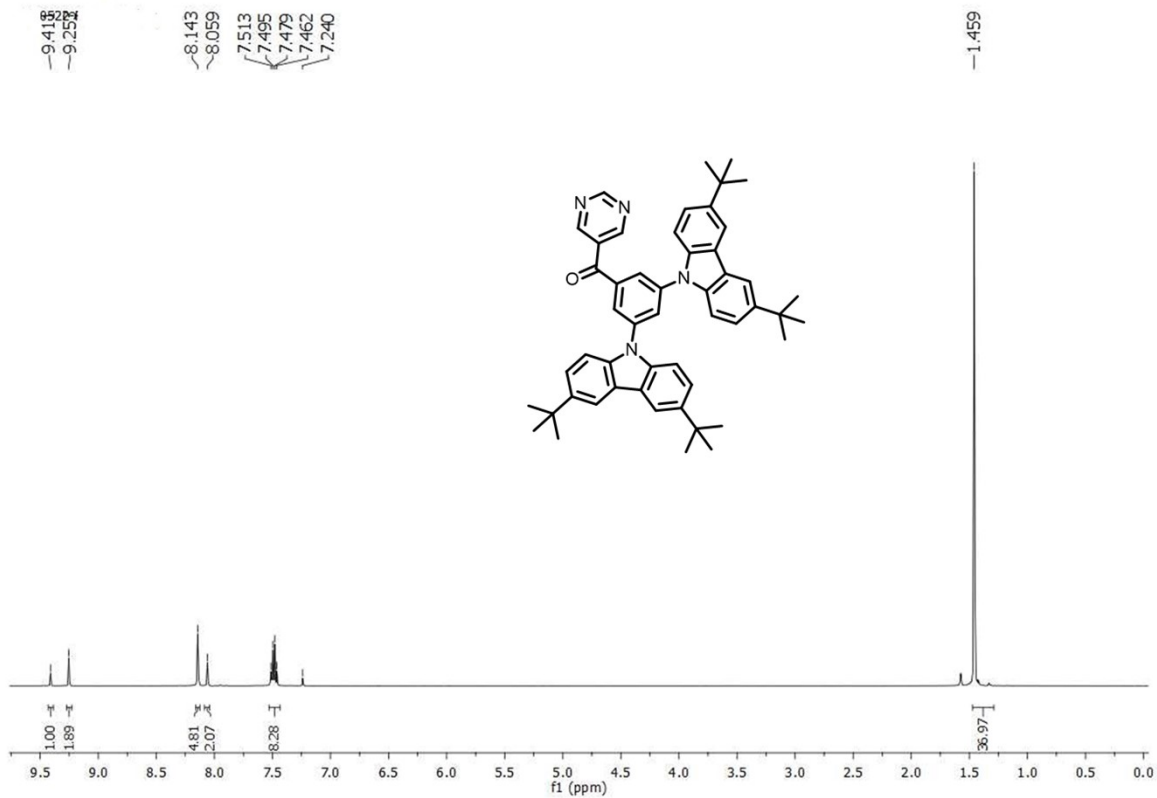
^{1}H AND ^{13}C Spectra of compound (25CzBPym)

¹H AND ¹³C Spectra of compound (25tCzBPym)

X-Ray crystallographic analysis:

General Crystal Growing Conditions: X-ray quality single crystals of **35CzBPym** and **25CzBPym,** were collected from the sublimed tube after cooling down to room temperature (sublimed temperatures are 210 and 215 ᵒC for **35CzBPym** and **25CzBPym** respectively).

ORTEP diagram of compound **35CzBPym (**CCDC = 1906824)
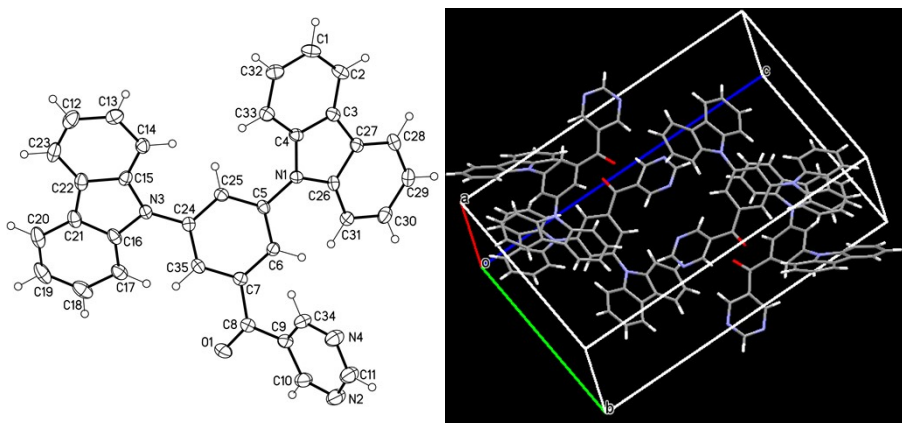
Crystal data and structure refinement for (35CzBPym).

Identification code	191047lt_0m
Empirical formula	C35 H22 N4 O
Formula weight	514.56
Temperature	100(2) K
Wavelength	0.71073 Å
Crystal system	Triclinic
Space group	P-1
Unit cell dimensions	a = 7.8835(5) Å α= 89.180(3)°.
	b = 15.0324(10) Å β= 86.928(3)°.
	c = 21.3072(14) Å γ = 83.005(3)°.
Volume	2502.6(3) Å^3
Z	4
Density (calculated)	1.366 Mg/m^3
Absorption coefficient	0.084 mm^{-1}

F(000)	1072
Crystal size	0.20 x 0.15 x 0.05 mm^3
Theta range for data collection	0.957 to 26.436°.
Index ranges	-9<=h<=9, -18<=k<=18, -26<=l<=26
Reflections collected	38234
Independent reflections	10009 [R(int) = 0.0277]
Completeness to theta = 25.242°	97.7 %
Absorption correction	Semi-empirical from equivalents
Max. and min. transmission	0.7454 and 0.6928
Refinement method	Full-matrix least-squares on F^2
Data / restraints / parameters	10009 / 0 / 721
Goodness-of-fit on F^2	1.128
Final R indices [I>2sigma(I)]	R1 = 0.0467, wR2 = 0.1290
R indices (all data)	R1 = 0.0649, wR2 = 0.1738
Extinction coefficient	n/a
Largest diff. peak and hole	0.545 and -0.468 e.Å^{-3}

ORTEP diagram of compound **25CzBPym** (CCDC = 1906825)
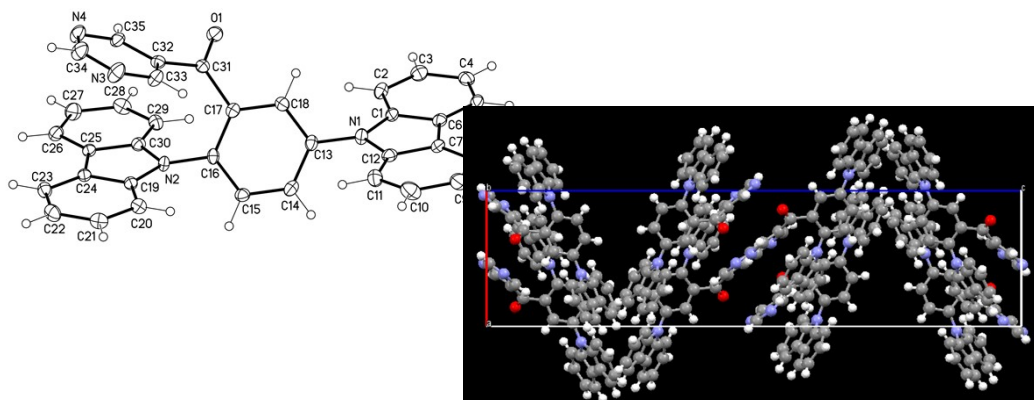
## Crystal data and structure refinement for (25CzBPym).

Identification code	180546LT_a

Empirical formula	C35 H22 N4 O
Formula weight	514.56
Temperature	100(2) K
Wavelength	0.71073 Å
Crystal system	Orthorhombic
Space group	P n a 21
Unit cell dimensions	a = 9.0970(3) Å $\alpha= 90°$.
	b = 15.4473(6) Å $\beta= 90°$.
	c = 35.8227(14) Å $\gamma = 90°$.
Volume	5034.0(3) Å^3
Z	8
Density (calculated)	1.358 Mg/m^3
Absorption coefficient	0.084 mm^{-1}
F(000)	2144
Crystal size	0.10 x 0.03 x 0.02 mm^3
Theta range for data collection	1.137 to 26.508°.
Index ranges	-11<=h<=9, -19<=k<=19, -44<=l<=44
Reflections collected	46967
Independent reflections	10371 [R(int) = 0.0371]
Completeness to theta = 25.242°	100.0 %
Absorption correction	Semi-empirical from equivalents
Max. and min. transmission	0.9485 and 0.8536
Refinement method	Full-matrix least-squares on F^2
Data / restraints / parameters	10371 / 1 / 721
Goodness-of-fit on F^2	1.048
Final R indices [I>2sigma(I)]	R1 = 0.0377, wR2 = 0.0829
R indices (all data)	R1 = 0.0518, wR2 = 0.0883
Absolute structure parameter	-0.3(5)
Extinction coefficient	n/a
Largest diff. peak and hole	0.205 and -0.224 e.Å^{-3}

Mass spectra of 35CzBPym

[Mass Spectrum]
Data : 2044   Date : 09-May-2018 16:19
RT : 2.18 min   Scan# : 49
Elements : C 36/0, H 30/0, N 4/0, O 1/0
Mass Tolerance   : 10ppm, 5mmu if m/z > 500
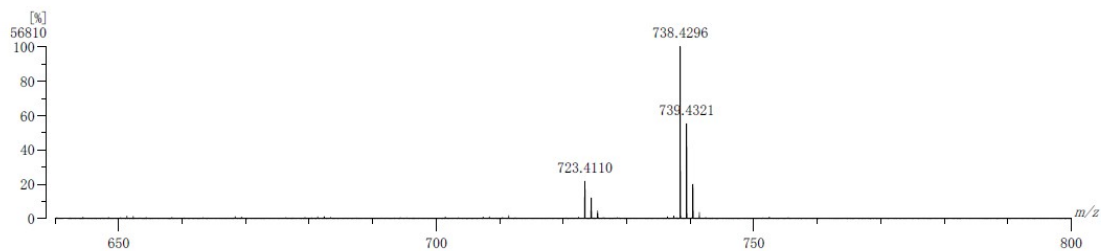Unsaturation (U.S.) : −0.5 − 35.0
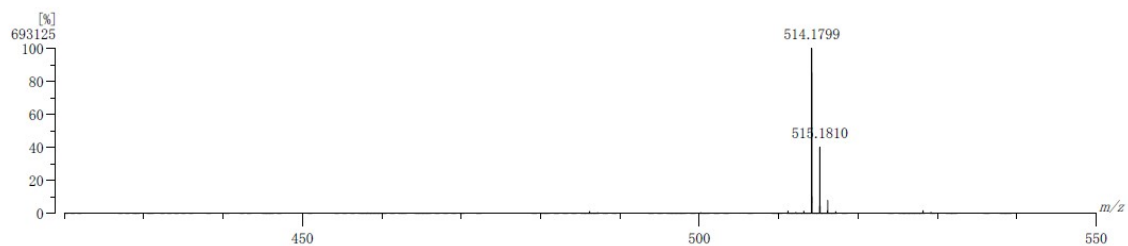
Observed m/z	Int%	Err[ppm / mmu]	U.S.	Composition
1 514.1799	100.00	+1.0 / +0.5	27.0	C35 H22 N4 O
515.1810	40.15			

Mass spectra of 35tCzBPym
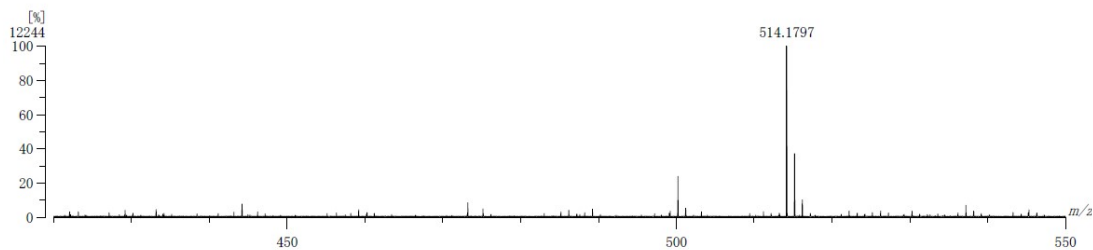
[Mass Spectrum]
Data : 2051   Date : 09-May-2018 17:31
RT : 0.89 min   Scan# : 24
Elements : C 52/0, H 70/0, N 4/0, O 1/0
Mass Tolerance   : 10ppm, 5mmu if m/z > 500
Unsaturation (U.S.) : −0.5 − 30.0

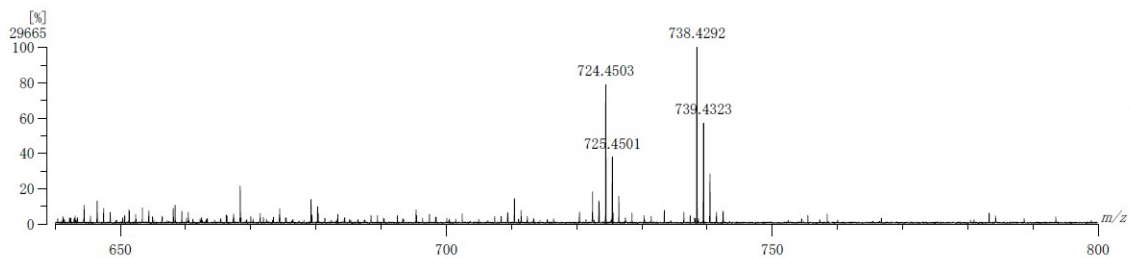| Observed m/z	Int%	Err[ppm / mmu]	U.S.	Composition
1 723.4110	21.73	+6.5 / +4.7	27.5	C50 H51 N4 O
2 738.4296	100.00	−0.2 / −0.2	27.0	C51 H54 N4 O
739.4321	55.25			
740.4335	20.04			

Mass spectra of 25CzBPym

[Mass Spectrum]
Data : 2046   Date : 09-May-2018 16:36
RT : 0.09 min   Scan# : 3
Elements : C 36/0, H 30/0, N 4/0, O 1/0
Mass Tolerance   : 10ppm, 5mmu if m/z > 500
Unsaturation (U.S.) : −0.5 ~ 30.0

Observed m/z   Int%   Err[ppm / mmu]   U.S. Composition
1   514.1797   100.00   +0.7 / +0.3   27.0   C35 H22 N4 O

Mass spectra of 25tCzBPym

[Mass Spectrum]
Data : 2050   Date : 09-May-2018 17:19
RT : 2.88 min   Scan# : (76,90)
Elements : C 52/0, H 70/0, N 4/0, O 1/0
Mass Tolerance   : 5ppm, 5mmu if m/z > 1000
Unsaturation (U.S.) : −0.5 ~ 30.0

Observed m/z   Int%   Err[ppm / mmu]   U.S. Composition
1   724.4503   78.78   −0.3 / −0.2   26.0   C51 H56 N4

2   725.4501   37.69   +4.1 / +3.0   25.5   C52 H57 N2 O

3   738.4292   100.00   −0.8 / −0.6   27.0   C51 H54 N4 O

     739.4323   56.99